Angle Diversity and Rate-Adaptive Transmission for Indoor Wireless Optical Communications

António Tavares, Rui Valadas, Rui L. Aguiar, and A. Oliveira Duarte
University of Aveiro and Institute of Telecommunications

ABSTRACT

The main degrading factor in indoor wireless optical communication systems for bit rates up to several megabits per second is the shot noise induced by ambient light (sunlight and artificial light produced by incandescent and fluorescent lamps). Due to the directional nature of both signal and ambient light noise, the spatial distribution of the signal-to-noise ratio in indoor environments can show large variations. This article compares techniques that are able to mitigate the effect of such SNR variations: rate-adaptive transmission and angle diversity. In the first technique, the effective data rate is adjusted to the local SNR conditions by introducing different levels of redundancy. The second technique explicitly explores the directionality of the SNR by combining signals collected from different observation angles. We address the performance of rate-adaptive transmission and angle diversity techniques, and compare them based on experimental results obtained in a typical indoor environment.

INTRODUCTION

Nondirected indoor wireless infrared communication systems were initially introduced by Gfeller and Bapst in [1]. Many developments have occurred since then [2–9], covering both point-to-point systems, such as Infrared Data Association (IrDA) devices [3], and local area networks, such as 802.11 [4], showing the vast potential of infrared technology. For wireless systems, infrared offers a major advantage over radio technologies: a large, virtually unlimited, bandwidth that is unregulated worldwide. Furthermore, infrared communications have inherent security characteristics, as infrared radiation is confined to closed rooms: there is no interference between contiguous systems operating in different rooms, and eavesdropping requires the attacking transceiver to be placed inside the room where the system is operating.

Wireless infrared communications are based on intensity modulation and direct detection of the optical carrier. Intensity modulation is performed by varying the current of a laser diode or an infrared LED. Direct detection is usually performed by PIN photodiodes, which produce an electrical current proportional to the incident optical power. For data rates up to several megabits per second, the major degrading factor in wireless infrared communications is the shot noise induced in the receiver by the ambient light [5], as ambient light sources (sunlight and artificial light) radiate in the same spectral wavelengths used by infrared transducers. The shot noise is larger when the receiver is placed under directional lamps and near windows exposed to sunlight. Furthermore, it can vary drastically during a normal day with the position of the sun and indoor lighting conditions [6]. The received signal can also vary significantly depending on the distance and the propagation conditions between the emitter and the receiver. Thus, the wireless infrared channel is characterized by large temporal and spatial variations of the signal-to-noise ratio (SNR). Typical infrared receivers do not easily accommodate these variations.

In this article we discuss techniques that can help mitigate the effect of the large SNR variations that may impair the indoor infrared wireless channel. In the first technique, rate-adaptive transmission [6, 10, 11], different levels of redundancy are introduced in the transmitted bit sequence to cope with the particular SNR conditions at the receiver site. The redundancy is accommodated by adjusting the effective data rate while keeping constant the symbol rate at the optical channel. If the receiver is located at a site with lower SNR, because of increased ambient light or obstruction in the propagation path, more redundancy is introduced in the transmitted bit sequence, leading to a decrease in the

effective data rate. We consider two methods of rate-adaptive transmission: repetition coding and binary convolutional coding. The second technique, angle diversity [7–9], explores the directional nature of both signal and noise. The SNR seen by a receiver can vary significantly with the observation angle. Clearly, if the receiver collects the signal and the noise from opposite directions, the SNR will be enhanced by orienting the optical collector to the direction of the signal while reducing its field of view (FOV). An angle diversity receiver is composed of multiple optical sectors with a relatively small FOV, each oriented to a different receiving angle. In this way, signals seen by different sectors will collect distinct SNRs and can be combined in order to increase the (output) SNR presented to the receiver. We consider several combination techniques: maximal ratio, select best, and equal gain. Angle diversity and rate-adaptive transmission techniques can also be used together to overcome the large temporal and spatial SNR variations.

AMBIENT LIGHT NOISE

The shot noise induced by ambient light determines, to a significant degree, the optical power budget required for reliable transmission. Thus, modeling the spatial distribution of the ambient light is important in order to accurately predict the system performance [5]. The shot noise variance is proportional to the dc photocurrent collected by a PIN photodiode. We consider now the case of incandescent and fluorescent illumination.

The dc photocurrent I_B produced by directional incandescent lamps can be modeled by the sum of two contributions: a generalized Lambertian source, accounting for the line-of-sight component, and an exponentially decaying factor, accounting for multiple reflections. Thus, with N directional incandescent lamps,

$$
\begin{aligned}
I_B \approx \sum_{i=1}^{N} \Bigg[& \Re \cdot \left(\frac{n_i + 1}{2\pi} P_i \frac{A_R}{h^2} \cos^{n_i} \beta_{E_i} \cos^3 \beta_{R_i} \right. \\
& \left. + \alpha P_i A_R e^{-\lambda d_{RE_i}} \right) \Bigg],
\end{aligned}
\tag{1}
$$

where, for the ith lamp, P_i is the emitted optical power, n_i is directly related to the half-power beamwidth of the lamp, β_{R_i} is the receiving angle (from the receiver normal), β_{E_i} is the emitting angle (from the lamp normal), and d_{RE_i} is the horizontal distance between the receiver and the lamp; moreover, h is the vertical distance between the receiver and the lamp, $\Re$ is the photodetector responsivity, A_R is the collecting area of the receiver, and α and λ are parameters that depend mainly on the room dimensions. Although not usually considered, practical evidence shows that the exponentially decaying factor accounting for multiple reflections is very important for close fitting of the spatial distribution of incandescent light environments.

For fluorescent illumination, units with parabolic reflectors containing two tubular lamps can be modeled by two linear arrays of several equally spaced generalized Lambertian sources. Thus, with N fluorescent units,

$$
I_B \approx \sum_{i=1}^{N} \sum_{j=1}^{M_i} \Bigg[\Re \cdot \left(\frac{n_{ij} + 1}{2\pi} P_{ij} \frac{A_R}{h^2} \cos^{n_{ij}} \beta_{E_{ij}} \right. \\
\left. \cos^3 \beta_{R_{ij}} + \right) \Bigg] + k,
\tag{2}
$$

where M_i is the number of Lambertian sources modeling the ith unit and the constant k accounts for multiple reflections. In practice, Lambertian sources spaced by 10 cm provide sufficient resolution.

We have characterized the spatial distribution of ambient light noise through measurements carried out in two indoor environments, one with incandescent and the other with fluorescent illumination. A PIN photodiode (VTH2091 from EG&G Vatec) with a collecting area of 0.85 cm^2 and a responsivity of 0.6 A/W at 850 nm was used. The dc photocurrent at the PIN photodiode was registered for a large set of positions within the rooms. The characteristics of the two test rooms are the following.

Room 1, with incandescent illumination, is a rectangular-shaped meeting room with large curtained windows on the east side and room dimensions 7.0 m × 5.0 m × 2.6 m (length × width × height). Measurements were performed during the night to neglect the contribution of natural light, which could emanate from windows. The measurement setup was placed 1.0 m above the floor. The illumination was very directional, being produced by nine spot lamps with narrow half-power beam widths (OSRAM, CONCENTRA SPC, R95, 100W). The location of the spot lamps were the following (in Cartesian coordinates relative to floor center): (–2.3, –1.8, 2.6), (–2.3, 0, 2.6), (–2.3, 1.8, 2.6), (0, –1.8, 2.6), (0, 0, 2.6), (0, 1.8, 2.6), (2.3, –1.8, 2.6), (2.3, 0, 2.6), and (2.3, 1.8, 2.6).

Room 2, with fluorescent illumination, is a rectangular-shaped laboratory darkroom. This room has no windows, and the room size is 6.0 m × 4.5 m × 3.1 m. The measurement setup was placed 0.9 m above the floor. The ambient light was produced by four fluorescent units with parabolic reflectors. Each fluorescent unit contains two 36 W tubular fluorescent lamps. The positions of the four units were (–1.7, –1.25, 3.1), (–1.7, 1.15, 3.1), (1.5, –1.25, 3.1), and (1.5, 1.15, 3.1).

Figure 1 illustrates both the measured and fitted spatial distributions of the dc photocurrents in the two rooms. Results show that there is a very good agreement between measured and fitted distributions, and also illustrate the large ambient noise variations that can impair indoor infrared wireless environments, especially when directional incandescent lamps are presented.

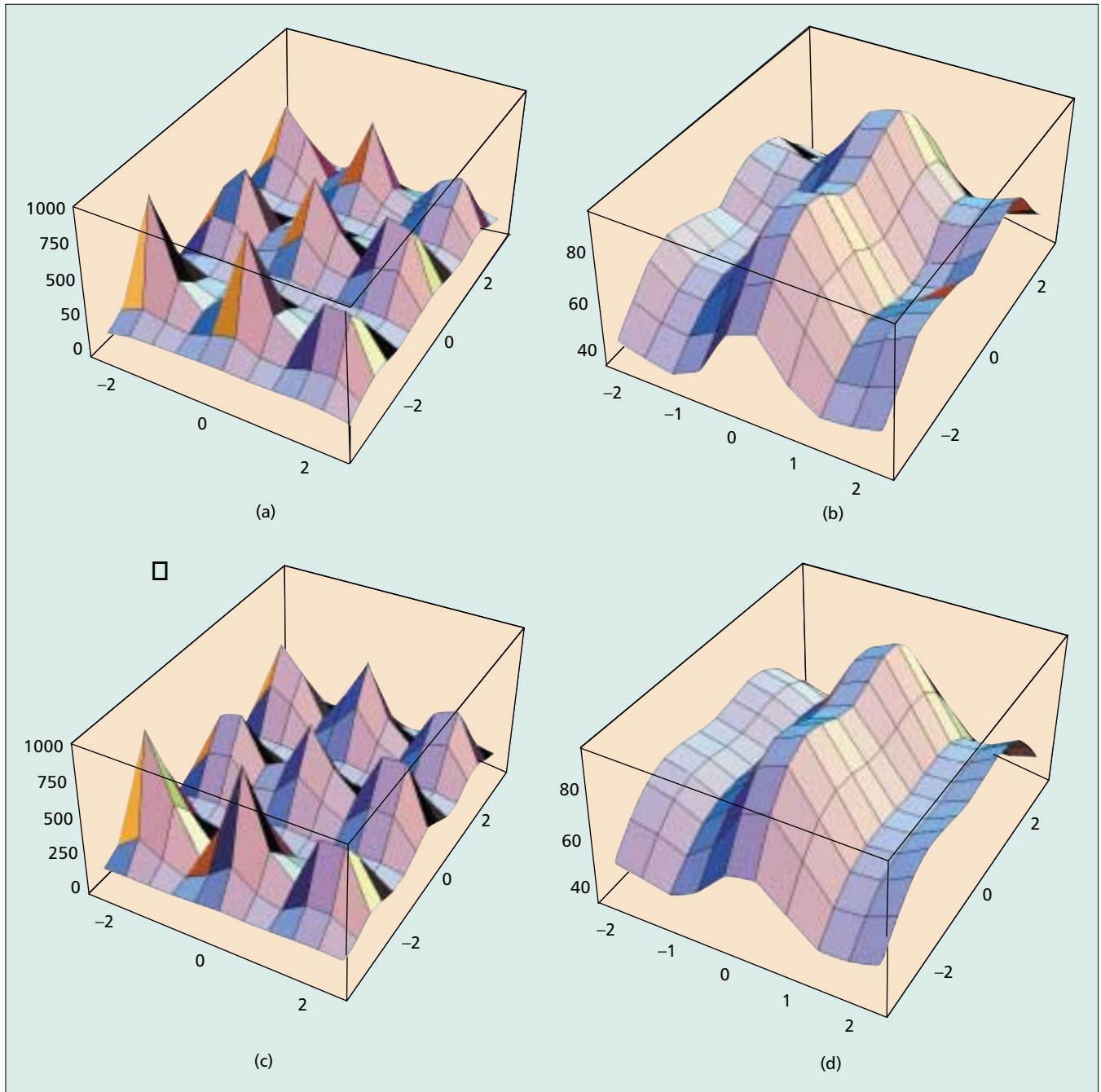## MULTIPLE DATA RATES IN 802.11 AND IRDA

There are presently two standardization bodies supporting worldwide standards for indoor wireless optical communication systems: the IEEE 802.11 group, created in July 1990, and IrDA, created in June 1993. While the focus of the IEEE 802.11 group was on nondirected indoor

Although not usually considered, practical evidence shows that the exponentially decaying factor accounting for multiple reflections is very important for close fitting of the spatial distribution of incandescent light environments.

optical wireless LANs, IrDA was mainly oriented to short-range low bit-rate line-of-sight systems. However, in recent years IrDA initiated a new project, called Advanced Infrared (AIr), whose main objective was to establish a new standard for nondirected optical wireless LANs. While the target system was similar for both AIr and IEEE 802.11, the two specifications present some differences, especially in the way multiple data rates are supported.

Both AIr and IEEE 802.11 specifications use pulse position modulation (L-PPM). The IEEE 802.11 standard supports two data rates. In order to keep the same pulse duration at the two data rates (250 ns), two different PPM schemes are used: 16-PPM at 1 Mb/s and 4-PPM at 2 Mb/s (Fig. 2). The physical layer header includes a field (3 bits) to distinguish between the different data rates. Maintaining the same pulse duration at the two data rates allows the system complexity to be minimized. In particular, the same receiver front-end can be used at both data rates. With the purpose of minimizing the hidden station problem, the same cell coverage is specified for 1 and 2 Mb/s. This requires approximately the same energy per symbol at 1 and 2 Mb/s. Since the pulse density of a 4-PPM signal is four times that of a 16-PPM signal, the average optical power emitted at 2 Mb/s is approximately 6 dB higher than the average optical power emitted at 1 Mb/s. Essentially, the support of two data rates in the

■ **Figure 1.** *Measured (top) and fitted (bottom) spatial distributions of the dc photocurrents (in μA/cm²) of two rooms illuminated by nine directional lamps, (a) and (c), and four fluorescent units, (b) and (d).*
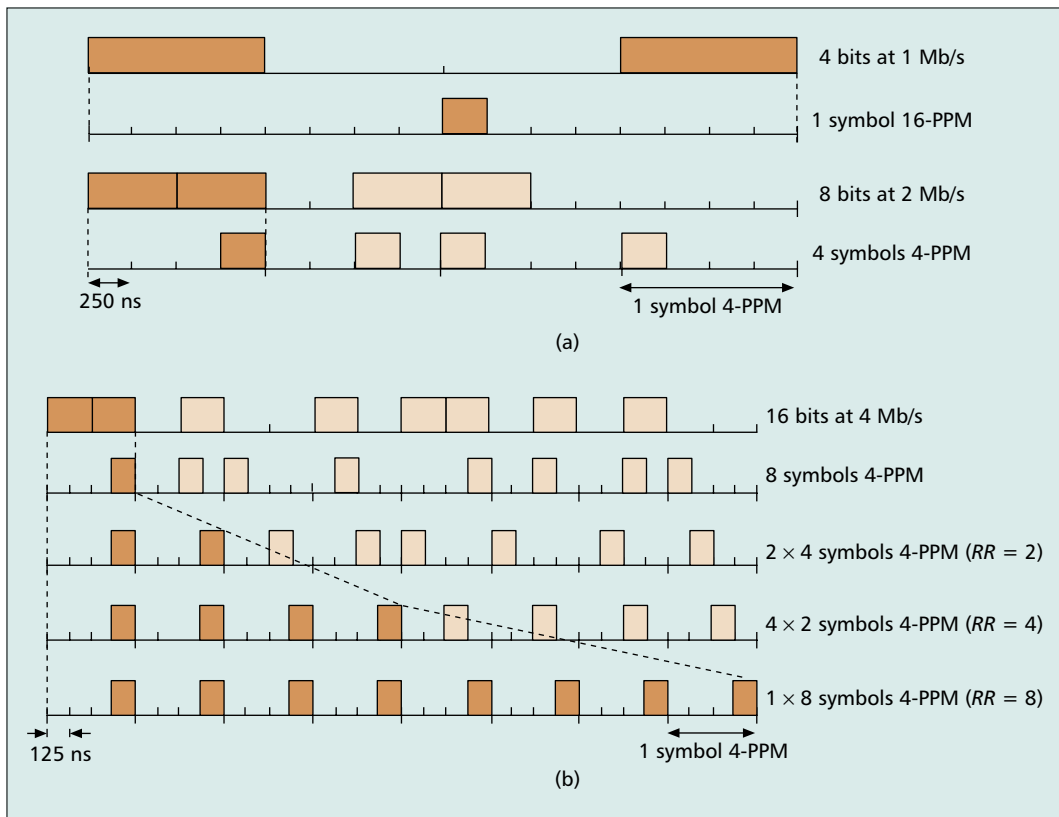
■ Figure 2. *Support of multiple data rates in: a) IEEE802.11; b) AIr specifications.*

IEEE 802.11 specification envisaged establishing trade-offs between data rate and power consumption.

AIr uses 4-PPM modulation at 4 Mb/s (i.e., with a pulse duration of 125 ns). It resorts to repetition coding in order to maintain connectivity over a large range of channel conditions. In this case, each 4-PPM symbol is repeated several times, which results in a reduction of the effective data rate (Fig. 2). According to the specification, rate reduction (RR) factors of 1, 2, 4, 8, and 16 can be accommodated, leading to effective data rates of 4 Mb/s, 2 Mb/s, 1 Mb/s, 500 kb/s, and 250 kb/s. Contrary to IEEE 802.11, the support of multiple (effective) data rates in AIr was motivated by the need to maintain connectivity at the largest possible set of indoor environments.

The medium access protocol of both AIr and IEEE 802.11 includes a reservation scheme to minimize the so-called hidden station problem. The source station, prior to sending data packets, exchanges Request-To-Send (RTS) and Clear-To-Send (CTS) mini-frames with the destination station. RTS and CTS broadcast information on the time interval that the channel will be occupied by the subsequent transmission (which can include several data packets). All stations, upon hearing the RTS or CTS frames, refrain from transmission until expiration of this reservation period. In the AIr specification the RTS/CTS exchange is also used to negotiate the data rate. Both RTS and CTS include a field (4 bits) that specifies the RR factor. The source station proposes a rate reduction in the RTS frame; the destination station, based on measurements carried out during reception of the RTS frame, answers indicating an adequate rate reduction to be used by the data packets.
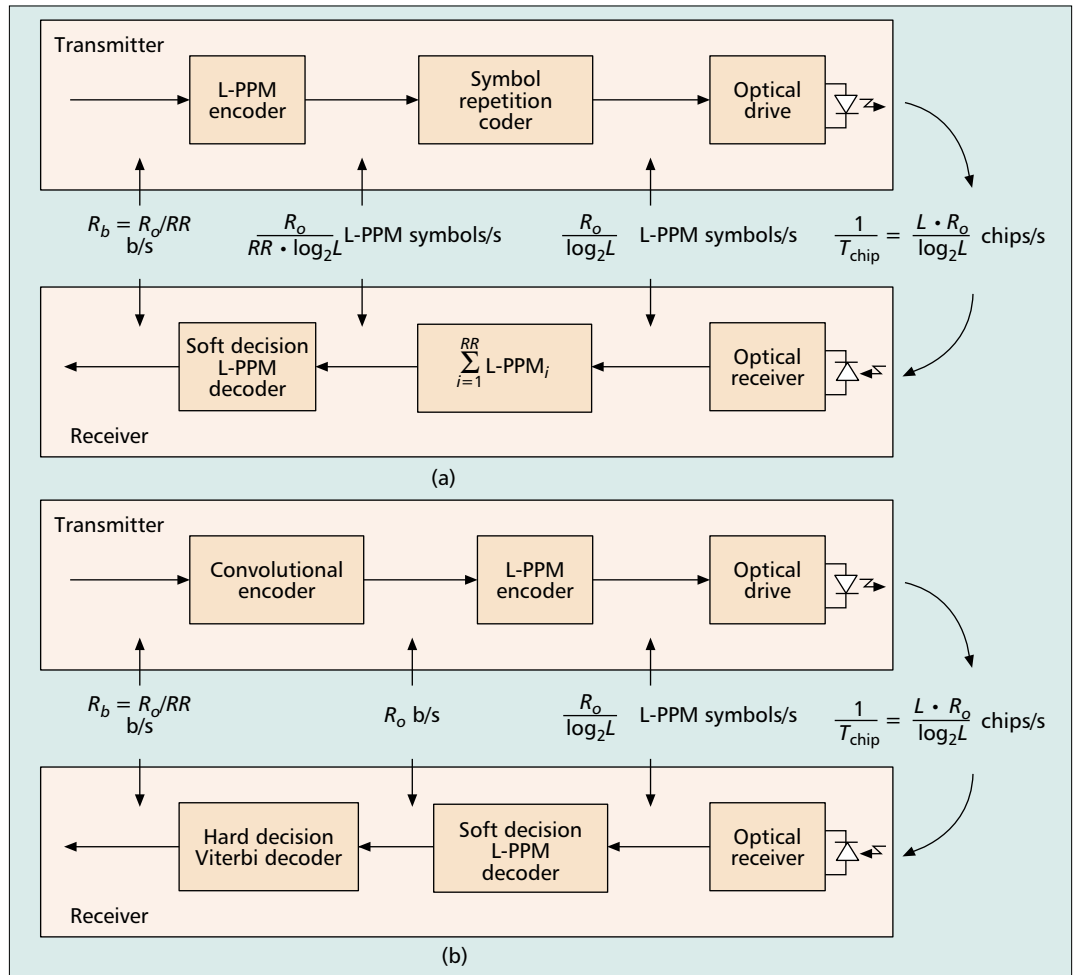
RATE-ADAPTIVE TRANSMISSION

We focus now on the performance of rate-adaptive transmission when applied to the wireless infrared channel. Besides repetition coding, which has been proposed for AIr, we also consider binary convolutional coding over L-PPM modulation.

REPETITION CODING

The repetition coding technique is based on the introduction of coding redundancy through the repetition of each L-PPM symbol. Figure 3a shows the block diagram of a repetition coding system that assumes L-PPM soft decision decoding. At the transmitter side, the L-PPM encoder converts each word with $\log_2 L$ bits, arriving at an effective data rate of $R_b = R_o/RR$ b/s, into an L-PPM symbol, where R_o is the maximum data rate. The repetition coding block repeats each L-PPM symbol RR times, leading to a chip rate that remains constant and equal to $LR_o/\log_2 L$, irrespective of RR. This allows a single receiving filter to be used at all (effective) data rates. At the receiver side the RR L-PPM symbols of the same block are summed together, and each resulting L-PPM is converted back to a word with $\log_2 L$ bits using soft decision decoding. In this way, the total chip energy is increased without increasing the chip duration, collecting area, or emitted optical power. Thus, the SNR is

■ Figure 3. *A block diagram of L-PPM rate-adaptive transmission systems with soft decision L-PPM decoding, employing: a) repetition coding; b) binary convolutional coding with hard decision Viterbi decoding.*

enhanced by virtual reduction of the receiving bandwidth. This technique is easily implemented without any changes in the front-end design. Assuming soft decision decoding, the bit error rate for repetition coding over L-PPM modulation is given by [12]

$$P_{RC} = \frac{L}{2(L-1)} \left\{ 1 - \frac{1}{\sqrt{2\pi}} \int_{-\infty}^{\infty} e^{-x^2/2} \right.$$
$$\left. \left[1 - Q\left(x + L\sqrt{2 \cdot RR \cdot \frac{\Re^2 P_{av}^2 T_{chip}}{\eta_o}} \right) \right]^{L-1} dx \right\}, \quad (3)$$

where $Q(k)$ is the tail probability of the Gaussian distribution, P_{av} is the average received power, T_{chip} is the chip duration, and η_o is the shot noise two-sided power spectral density. For a specific bit error rate, doubling RR decreases the required SNR by 3 electrical dB.

BINARY CONVOLUTIONAL CODING

The second rate-adaptive transmission technique uses convolutional coding. This technique differs from the previous one because it allows error correction at the receiver. Several convolutional codes with code rates $R_C = k/n$ can be used [10, 11], where n is the number of output bits for each input word with k bits. In order to enable direct comparison between the two rate-adaptive transmission systems, $1/R_C$ is constrained to be an integer. Due to implementation complexity considerations, we take $k = 1$ and $n = RR$.

Figure 3b shows the block diagram of a binary convolutional coding system. At the transmitter side, the convolutional encoder converts each bit ($k = 1$), arriving at an effective data rate of $R_b = R_o/RR$ b/s, into a codeword with $n = RR$ bits. The bit sequence is then L-PPM modulated and transmitted in the channel at a chip rate equal to that of the repetition coding system. This will allow directly comparing the performance of the two rate-adaptive transmission systems. The processing at the receiver includes soft decision L-PPM demodulation followed by hard decision Viterbi decoding. This is one of several possibilities.

The choice of the best convolutional codes is a compromise between complexity and performance. Higher constraint lengths (number of stages in the encoder), K, do produce better performances but increase the complexity of the decoding process. When a binary convolutional code with constraint length K is decoded by means of the Viterbi algorithm, there are 2^{K-1} states. Hence, there are 2^{K-1} surviving paths at each stage and 2^{K-1} metrics, one for

each surviving path. Thus, the number of computations required at each stage increases exponentially with K, which limits the use of the Viterbi algorithm to relatively small values of K [12]. Further limitations are imposed by the system bit rate. Based on practical experience, we have considered $K = 3, 4, 5$. The best codes for $n = 2, 4, 8, 16, 32$ and $K = 3, 4, 5$ are listed in Table 1 [10]. Clearly, the complexity of a binary convolution coding system can be much higher than that of a repetition coding system. Assuming hard decision Viterbi decoding, an upper bound on the bit error probability is given by [12]

$$P_{CC} \le \sum_{d=d_{free}}^{\infty} \beta_d \left[4 P_{RC} \left(1 - P_{RC} \right) \right]^{d/2}, \qquad (4)$$

where P_{RC} is the bit error probability given by Eq. 3 with $RR = 1$.
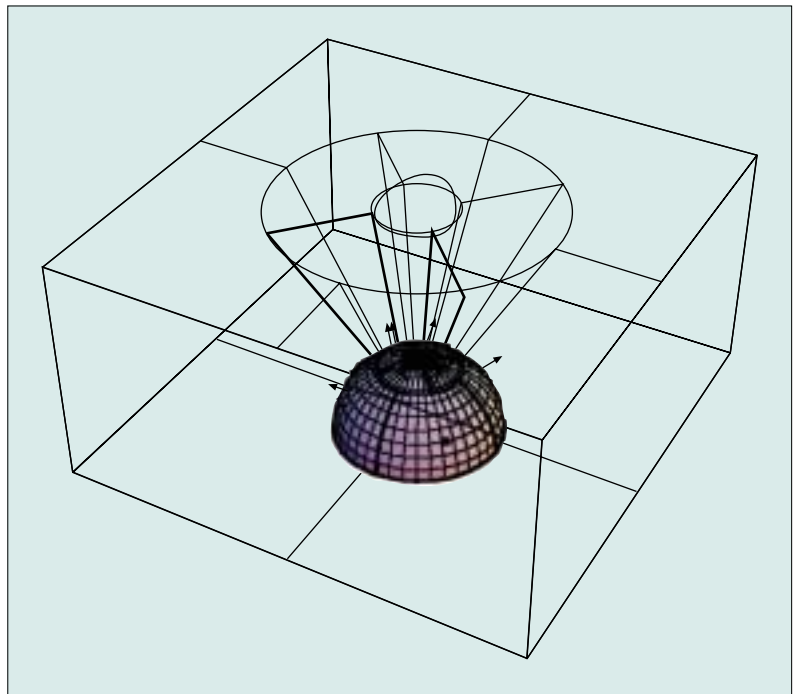
ANGLE DIVERSITY

Receivers for IR communications are usually based on a single optical detector with a large FOV. A detector with a wide FOV may collect a large percentage of undesired ambient light together with the desired optical signal. This is a good configuration in environments where both signal and noise are isotropic, which is not the usual case. Due to the directional nature of both signal and noise, the SNR can vary significantly, depending on:
• The position, orientation, and radiation pattern of both signal and noise sources
• The position, orientation, and FOV of the receiver
In such an environment, significant performance improvements have been demonstrated [7–9] by using angle diversity receivers. An angle diversity optical receiver can be defined as a set of optical receivers (sectors) with relatively small FOV that point in different directions. The receiver operates by estimating the SNR seen by each sector and combining the signals collected in each sector in order to improve the output SNR. We note that angle diversity can be applied to both IEEE 802.11 and IrDA systems.

OPTICAL STRUCTURE
The FOV of an angle diversity receiver can be modeled based on a hemisphere where the sectors are delimited by a set of parallels and equally spaced meridians [7], as represented in Fig. 4. The region of the sectored receiver enclosed between two parallels defines a segment. The sectored receiver FOV is defined by four surfaces: two surfaces with a constant azimuth and two surfaces with a constant elevation. Thus, the FOV of a sector is completely determined by two limiting elevation angles θ_l and θ_h with $\theta_l < \theta_h$, and two limiting azimuth angles φ_l and φ_h with $\varphi_l < \varphi_h$. The configuration of the sectored receiver is completely specified by a set Ψ where each subset corresponds to one of the segments of the receiver. Each subset has four elements indicating the number of sectors, the azimuth offset of the first sector φ_o, and the limiting elevation angles θ_l and θ_h of the segment. The azimuth aperture, $\varphi_h - \varphi_l$, is the same for all sec-
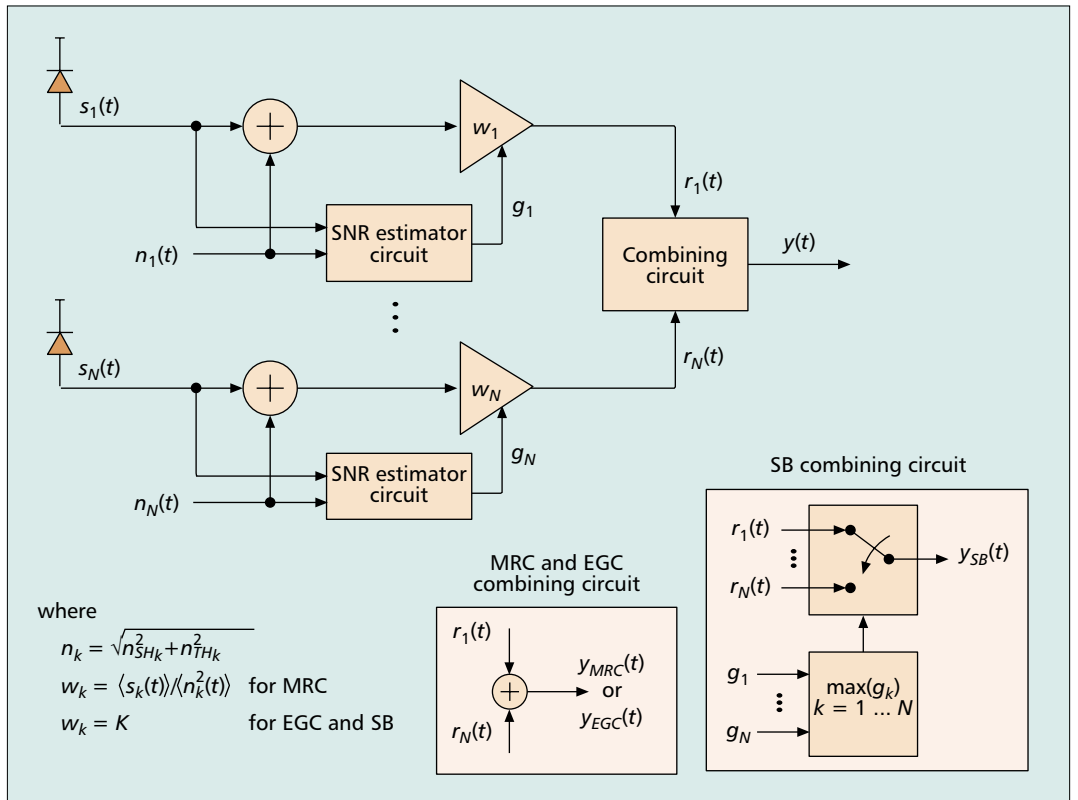

■ **Figure 4.** *The angle diversity receiver model.*

Rate	K	Generators (octal)	d_{free}
1/2	3	5, 7	5
	4	15, 17	6
	5	31, 35	7
1/4	3	5, 7*3	10
	4	13, 15*2, 17	13
	5	25, 33, 35, 37	16
1/8	3	5*3, 7*5	21
	4	13, 15*4, 17*3	26
	5	25*2, 33*2, 35*2, 37*2	32
1/16	3	5*5, 7*11	42
	4	13*2, 15*9, 17*5	53
	5	25*4, 33*4, 35*4, 37*4	64
1/32	3	5*11, 7*21	85
	4	13*3, 15*18, 17*11	106
	5	25*8, 33*8, 35*8, 37*8	128

■ **Table 1.** *Parameters of the best convolutional codes with rate 1/n for n = 2, 4, 8, 16, 32 and K = 3, 4, 5.*

tors belonging to the same segment. The sectored receiver represented in Fig. 4 is specified by $\psi = \{\{1,0°, 0°, 10°\}, \{4,45°, 10°, 30°\}, \{4,0°, 30°, 90°\}\}$. It has three segments and a total of nine sectors.

COMBINING TECHNIQUES
An angle diversity receiver operates by amplifying, separately, the photocurrents received in the various sectors. The resulting electrical signals can be processed in one of several ways, depending on the combination technique employed: select best (SB), maximal ratio combining (MRC), and equal gain combining (EGC). The structure of an angle diversity

■ Figure 5. *Combining techniques in angle diversity receivers.*

receiver is represented in Fig. 5. In the case of an SB technique the combining circuit works as an analog multiplexer that selects the sector with the highest SNR. For the MRC receiver the combining circuit implements a weighted summation according to the SNR of the sector. Finally, in the EGC combining alternative, the outputs of the diversity branches are weighted equally before being summed to give the resulting output.

The SB combining technique improves the SNR by choosing the optical sector with the highest SNR only. When there is no correlation between the noise of the sectors, the optimum output SNR is achieved by the MRC strategy. In an MRC receiver, signals from N sectors are combined using weights directly proportional to the ratio of incident optical power to noise variance. The output SNR obtained using an MRC receiver corresponds to the effective summation of the SNR of all sectors. In an EGC receiver, the output SNR corresponds to the ratio of the squared sum of photodiode currents to the sum of noise variances.

Although the EGC combining technique does not directly explore the directionality of signal and noise, there are two main reasons for considering its utilization. First, the SNR is increased by about 3 dB with duplication of the number of sectors if the received optical power is constant and the shot noise is induced by a steady background light. Second, this technique allows the effective collecting area to be increased without the associated loss of bandwidth, since the junction capacitance of the photodetector is not increased.

PERFORMANCE EVALUATION

REPETITION CODING VS. CONVOLUTIONAL CODING

In order to compare repetition and convolutional coding, we consider 4-PPM modulation with maximum data rate $R_o = 4$ Mb/s, $n = RR = 1$, 2, 4, 8, 16, and 32, corresponding to effective data rates of 4 Mb/s down to 125 kb/s, and convolutional codes with $K = 3$, 4, and 5. Figure 6 compares the performance of the various schemes. The graph shows the average power gain (at a bit error rate of 10^{-9}) over a reference
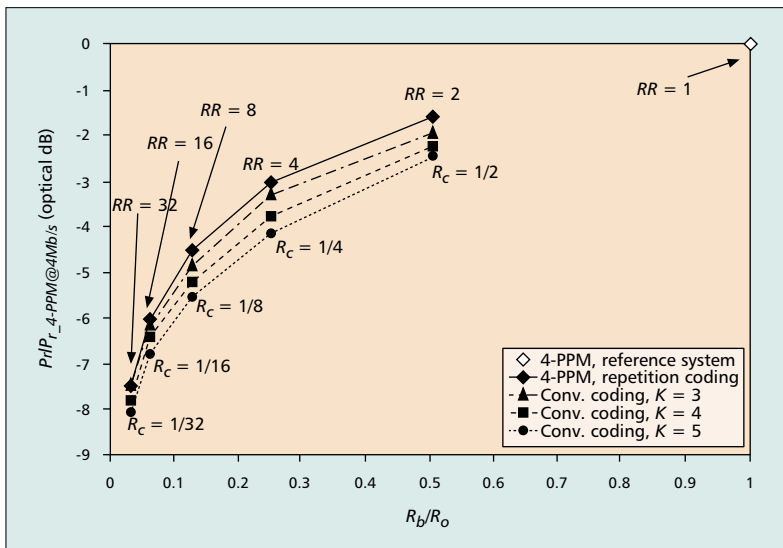
■ Figure 6. *Optical power gains of repetition coding and binary convolutional coding.*
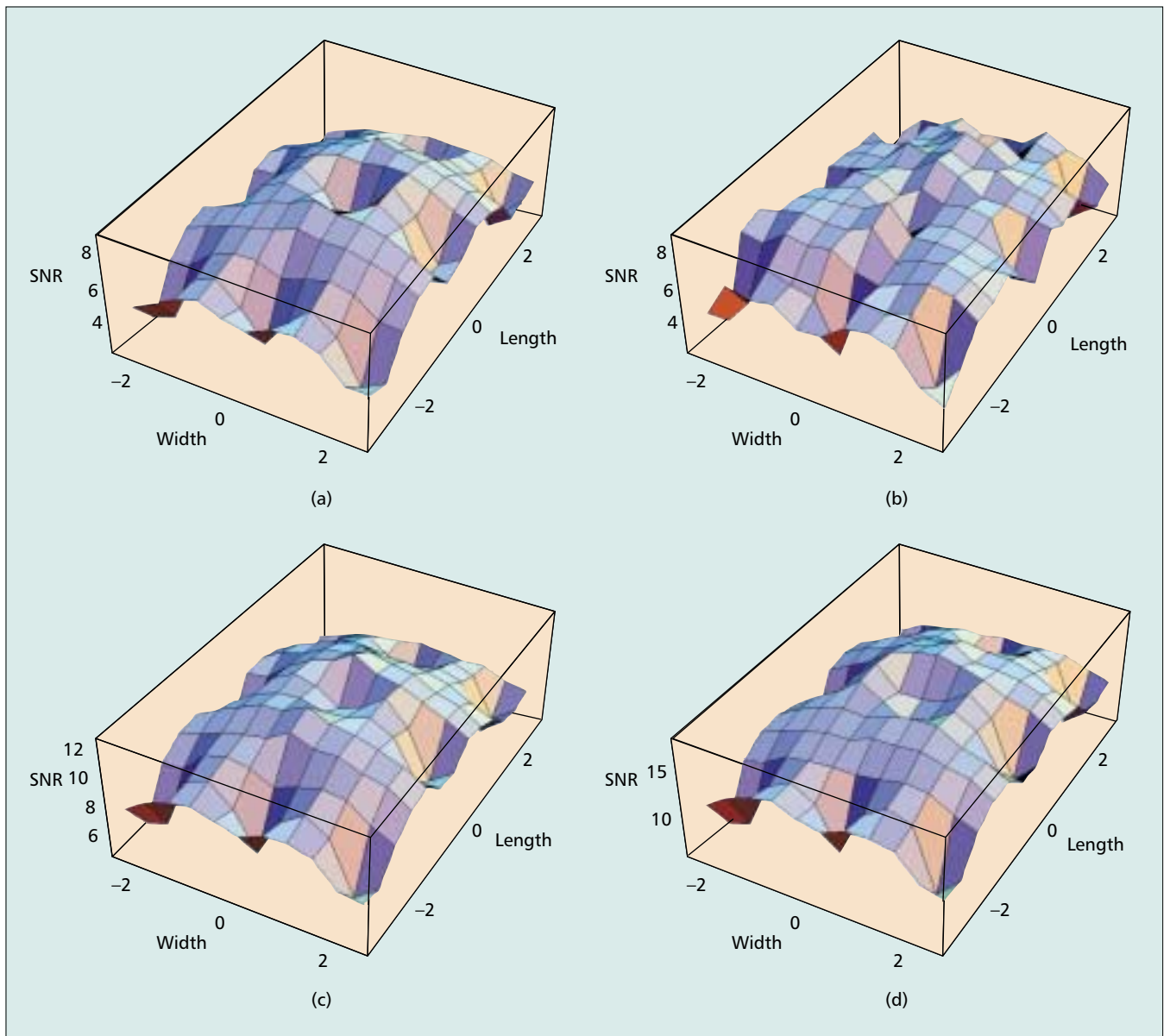
Figure 7. *Measured spatial SNR distribution of: a) nonsectored; b) SB; c) EGC; d) MRC receivers.*

system with $n = RR = 1$ vs. the normalized bit rate R_b/R_o. In the repetition coding system, doubling RR produces an optical power gain of 1.5 dB; similarly, reducing the code rate of the convolutional coding system by a factor of 2 produces optical power gains close to 1.5 dB. The gains of convolutional coding over repetition coding tend to decrease for lower code rates. The main improvements of the convolutional code with higher K over repetition coding varies from about 0.56 to about 1.11 dB. The gains over the reference system range from 2.37 dB (rate 1/2) to about 8.09 dB (rate 1/32) for convolutional coding, while for repetition coding these gains vary from 1.5 dB to 7.5 dB. It can be concluded that in order to ensure significant gains over the whole range of rate reduction factors, the constraint length of convolutional coding needs to be at least 4 or 5. Thus, it may not be worthwhile to use convolutional coding, given that the implementation complexity can be significantly higher.

ANGLE DIVERSITY COMBINING TECHNIQUES

In order to study the performance of angle diversity, we have developed three laboratory prototypes, each implementing a different combining technique (SB, EGC, and MRC) with a common optical configuration defined by $\psi = \{\{8,0°, 0°, 90°\}\}$. The system was tested in rooms 1 and 2 described above. A summary of the performed measurements is listed in Table 2. The measurements were carried out using a wide-bandwidth 86100A Agilent infiniium digital communication analyzer prepared to estimate the SNR. In both illumination scenarios, the MRC strategy achieved the best results (i.e., the highest minimum SNR) with significant gains over a nonsectored receiver. The gains with the EGC strategy were also high. However, the SB strategy showed a penalty relative to the nonsectored receiver, which can be attributed to the relatively low number of sectors. This also explains the lack of improvement in terms of SNR range, which was

■ **Table 2.** *SNR measurements of nonsectored, SB, EGC, and MRC receivers.*

It is interesting to note that there may be loss of connectivity or lower effective data rate at the room center due to the spot lamp that is positioned at the ceiling center.

expected to be higher. Note that the number of sectors is lower than the number of incandescent spot lamps in room 1. The gains achieved with the MRC and EGC strategies were 3.96 dB and 1.61 dB, respectively, in room 2 (fluorescent illumination), and 6.61 dB and 5.09 dB, in room 1 (incandescent illumination). As an example, we present in Fig. 7 the detailed SNR measurements of room 1.

REPETITION CODING VS. ANGLE DIVERSITY

We consider now the connectivity areas obtained with repetition coding and angle diversity techniques in the same conditions of the previous section, for the case of a room illuminated with incandescent lamps. The criteria for defining the connectivity areas was a bit error rate of 10^{-9}. The bit error rate achieved with the laboratory prototype at all receiver positions was measured using an ANRITSU ME522A error rate measurement

system. The connectivity areas are depicted in Fig. 8. In Figs. 8a–d, the lightest zones indicate connectivity at 4 Mb/s and the darkest zones loss of connectivity due to excessive bit error rate. Figure 8e, corresponding to the repetition coding system, shows that full connectivity is maintained at all room locations by decreasing the effective data rate from 4 to 1 Mb/s (darker areas mean a lower bit rate). It is interesting to note that there may be loss of connectivity or lower effective data rate at the room center due to the spot lamp positioned at the ceiling center. With the nonsectored, SB, EGC, and MRC receivers connectivity is achieved in 66.4, 65.7, 93.0, and 99.3 percent of the room area, respectively. With the repetition rate system, transmission is at 4 Mb/s in 66.4 percent of the room, 2 Mb/s in 25.9 percent of the room, and 1 Mb/s in 7.7 percent of the room. Clearly, the combination of MRC or EGC angle diversity and repetition coding yields a very high
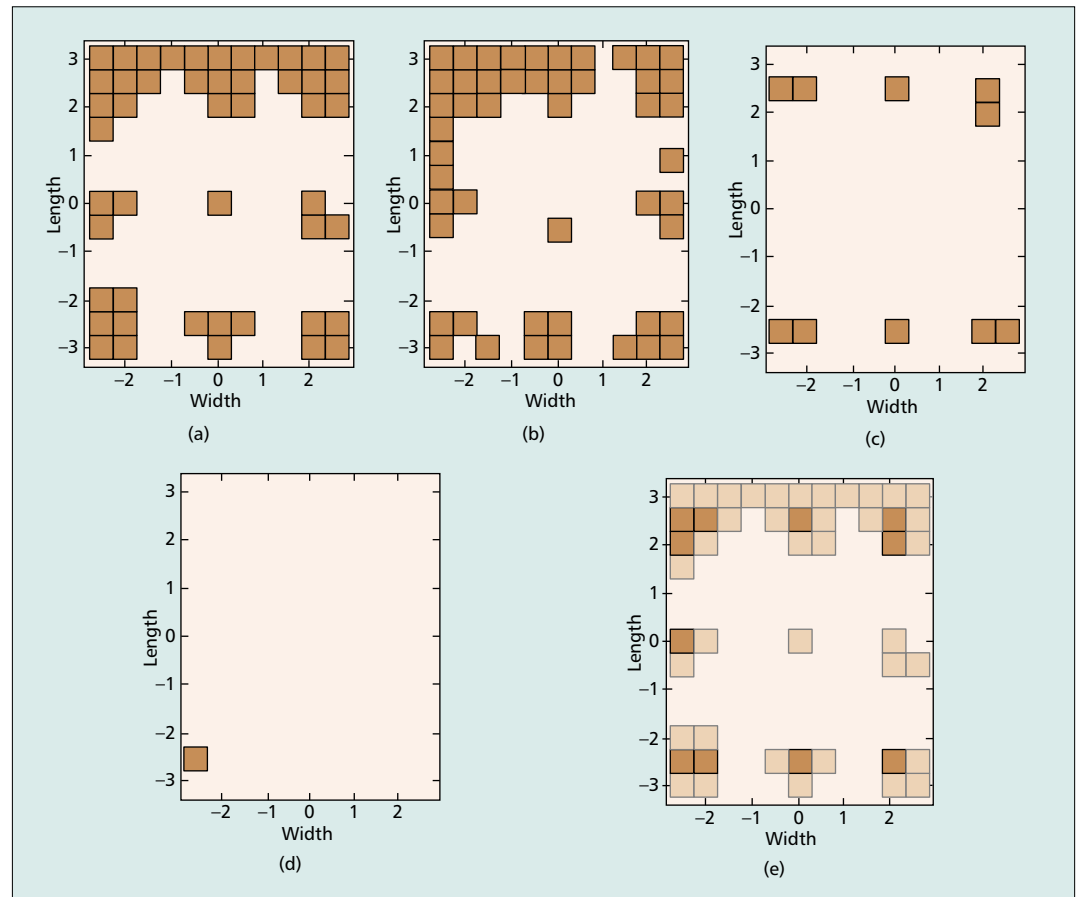
■ **Figure 8.** *Connectivity areas of: a) reference system (nonsectored receiver and RR = 1); b) SB receiver; c) EGC receiver; d) MRC receiver; e) repetition coding system.*

performance system capable of overcoming the large SNR variations of the indoor wireless infrared channel.

Conclusions

We have compared rate-adaptive transmission and angle diversity as techniques to overcome the large SNR variations of the indoor optical wireless channel. Performance evaluation of both techniques was carried out experimentally on typical indoor environments. The results show that the techniques are very effective, allowing connectivity to be maintained despite large SNR variations. If maximum throughput at a large percentage of the cell area is required, angle diversity needs to be implemented. However, even then there may be zones where connectivity is completely lost. Thus, a robust system, simultaneously achieving throughput maximization and graceful throughput degradation, may require the implementation of both angle diversity and rate-adaptive transmission techniques.

References

[1] F. Gfeller and U. Bapst, "Wireless In-House Data Communication via Diffuse Infrared Radiation," *Proc. IEEE*, vol. 67, no. 11, Nov. 1979, pp. 1474–86.
[2] J. Kahn and J. Barry, "Wireless Infrared Communications," *Proc. IEEE*, vol. 85, no. 2, Feb. 1997, pp. 265–98.
[3] S. Williams, "IrDA: Past, Present and Future," *IEEE Commun. Mag.*, Feb. 2000, pp. 11–19.
[4] R. Valadas *et al.*, "The Infrared Physical Layer of the IEEE 802.11 Standard for Wireless Local Area Networks," *IEEE Commun. Mag.*, Dec. 1998, pp. 2–7.
[5] A Tavares, R. Valadas, and A. Duarte, "Performance of Wireless Infrared Transmission Systems Considering Both Ambient Light Interference and Intersymbol Interference Due to Multipath Dispersion," *Opt. Wireless Commun.*, *Proc. SPIE*, vol. 3532, Boston, MA, Nov. 1998, pp. 82–93.
[6] F. Gfeller *et al.*, "Dynamic Cell Planning for Wireless Infrared In-House Data Transmission," *Int'l. Zurich Sem. Dig. Commun.*, Zurich, Switzerland, Mar. 1994, pp. 261–72.
[7] R. Valadas, A. Tavares, and A. Duarte, "Angle Diversity to Combat the Ambient Noise in Indoor Optical Wireless Communication Systems," *Int'l. J. Wireless Info. Networks*, vol. 4, no. 4, Plenum Press, Oct. 1997, pp. 275–88.
[8] J. Kahn *et al.*, "Imaging Diversity Receivers for High-Speed Infrared Wireless Communications," *IEEE Commun. Mag.*, vol. 36, Dec. 1998, pp. 88–94.
[9] J. B. Carruthers and J. M. Kahn, "Angle Diversity for Nondirected Wireless Infrared Communications," *IEEE Trans. Commun.*, vol. 48, no. 6, June 2000.
[10] R. Alves and A. Gameiro, "Coding of PPM Based Modulation Techniques to Improve the Performance of Infrared WLANs," *Proc. IEEE-Fall VTC*, 2000, pp. 1345–52.
[11] L. Diana and J. Kahn, "Rate-Adaptive Modulation Techniques for Infrared Wireless Communications," *Proc. IEEE ICC*, vol. 1, Vancouver, Canada, June 6–10, 1999, pp. 597–603.
[12] J. Proakis, *Digital Communications*, 3rd ed., New York: McGraw-Hill, 1995, pp. 470–511.

Biographies

ANTONIO R. TAVARES (tavares@det.ua.pt) received a Licenciatura degree in electronics and telecommunications engineering from the University of Aveiro, Portugal, in 1991. Just after graduation, from 1991 to 1993, he joined the Broadband Communications Systems Research Group at the same university where he worked in indoor wireless optical communications. He joined the University of Aveiro in 1999, where he is now an invited lecturer in the Department of Electronics and Telecommunications. He is currently working toward a Ph.D. degree in electrical engineering at the University of Aveiro. He is also a researcher at the Institute of Telecommunications, Aveiro, Portugal. His current research interests include several indoor wireless optical communications issues: modulation methods, angle diversity receivers, and the characterization of optical noise and interference due to ambient light.

RUI T. VALADAS (rv@det.ua.pt) received a Licenciatura degree from Instituto Superior Técnico, Lisbon, Portugal, in 1986 and a Ph.D. degree from the University of Aveiro, Portugal, in 1996. He joined the University of Aveiro in 1986, where he is now an associate professor in the Department of Electronics and Telecommunications. He is also a researcher at the Institute of Telecommunications, Aveiro, Portugal. He participated in the specification of the IEEE 802.11 "Wireless Access Method and Physical Layer Specification" standard. His main research interests are in the areas of wireless optical networks and traffic engineering for multiservice networks.

RUI L. AGUIAR (ruilaa@det.ua.pt) received a Licenciatura degree in electronics and telecommunications engineering, an M.Sc. degree in microelectronics for telecommunications, and a Ph.D. degree in electrical engineering in 1990, 1995, and 2001 from the University of Aveiro, Portugal. He is currently an assistant professor in the Electronics and Telecommunications Department of the University of Aveiro, teaching electronics and networking subjects. He is also a researcher at the Institute of Telecommunications, Aveiro, Portugal. His current research interests are centered on the implementation of advanced wireless networks and systems, with special emphasis on high bit rates and QoS aspects.

A. MANUEL DE OLIVEIRA DUARTE (duarte@ua.pt) is a full professor with the Department of Electronics and Telecommunications, University of Aveiro, Portugal, which he joined in 1978. He received a Licenciatura degree in electrical engineering from the University of Coimbra in 1976, and M.Sc. and Ph.D. degrees in telecommunications systems and Electrical engineering sciences in 1981 and 1984 from the University of Essex, United Kingdom. In 1988 he created the Broadband Systems Group of the University of Aveiro which, over the years, diversified into a series of interrelated research teams acting in the areas of broadband technologies, optical wireless networks, teletraffic, organization and structure of telecommunications networks and services, and economic and social aspects of telecommunications. More recently, he has been put in charge of several educational and vocational training programs of the University of Aveiro in the areas of industrial design, production technologies, and management.

A robust system, simultaneously achieving throughput maximization and graceful throughput degradation, may require the implementation of both angle diversity and rate-adaptive transmission techniques.